

# Stability and gas sensing properties of $Ta_2X_3M_8$ ( $X = Pd, Pt$ ; $M = S, Se$ ) nanoribbons by first-principles investigation

## Supporting information

**Ekaterina V. Sukhanova<sup>1,2,3</sup>, Maxim A. Visotin<sup>4,5</sup>, Zakhar I. Popov<sup>1,3</sup> and Pavel B. Sorokin<sup>1,2,\*</sup>**

<sup>1</sup> National University of Science and Technology MISiS, 4 Leninskiy prospekt, Moscow, 119049, Russian Federation

<sup>2</sup> Moscow Institute of Physics and Technology (State University), 9 Institutskiy per., Dolgoprudny, Moscow Region, 141701, Russian Federation

<sup>3</sup> Emanuel Institute of Biochemical Physics of RAS, 4 Kosygin Street, Moscow, 119334, Russian Federation

<sup>4</sup> Kirensky Institute of Physics, Federal Research Center KSC, Siberian Branch, Russian Academy of Sciences, Akademgorodok, Krasnoyarsk, 660036, Russian Federation

<sup>5</sup> Siberian Federal University, Krasnoyarsk, 660041, Russian Federation

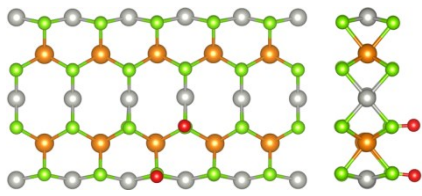
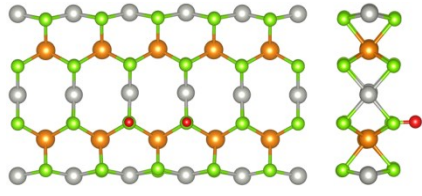
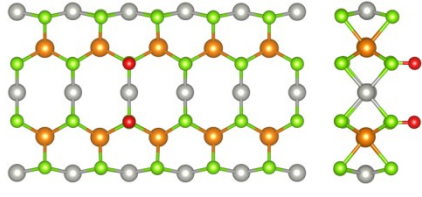
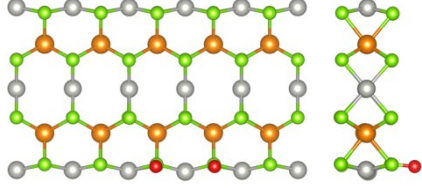
\*Corresponding author: e-mail [pbsorokin@misis.ru](mailto:pbsorokin@misis.ru)

## SI. Considered configurations of two adsorbed oxygen atoms on the nanoribbons surface and of chalcogen monovacancy.

Five different oxygen positions were considered for two adsorbed oxygen atoms on the nanoribbons surface (Table S1): the first oxygen atom was situated at the edge of the ribbon, the second atom was in the center, both atoms were on the front side of the NR (4-6), both oxygen atoms were located above the neighboring chalcogen atoms in the center of the nanoribbon, both chalcogen atoms lie on the one line of atoms (4-4'), both oxygen atoms were above the chalcogen atoms in the center of the NR, chalcogen atoms lie on different lines of atoms (4-10), both oxygen atoms were located above adjacent chalcogen atoms on the edge of the nanoribbon (6-6'), and both oxygen atoms were on the backside of the nanoribbon (9-9'').

Two different positions of chalcogen vacancy were considered (Table S2): in the center (4) and at the edge (6) of the nanoribbon.

Table S1. Energy difference between the second and the first steps of TPS nanoribbons oxidation reaction.

Structure	Atomic structure	$E_2 - E_1$ , eV			
		$\text{Ta}_2\text{Pd}_3\text{S}_8$	$\text{Ta}_2\text{Pd}_3\text{Se}_8$	$\text{Ta}_2\text{Pt}_3\text{S}_8$	$\text{Ta}_2\text{Pt}_3\text{Se}_8$
4-6		-1.22	0.52	-1.15	0.59
4-4'		-1.17	0.44	-1.11	0.44
4-9		-1.17	0.46	-1.07	0.55
6-6'		-1.28	0.60	-1.17	0.80

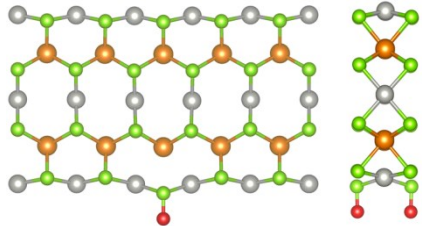
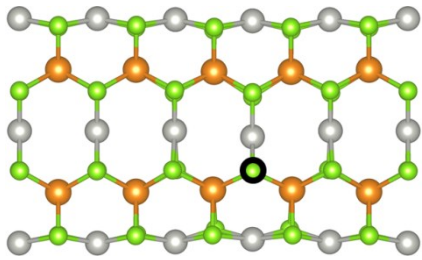
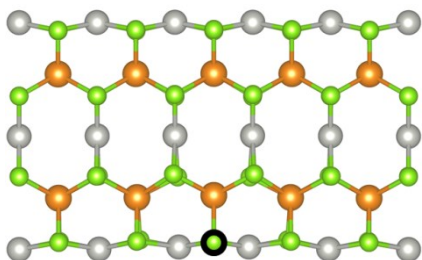
5-5''		-0.15	0.75	-0.46	0.42
-------	---	-------	------	-------	------

Table S2. Energy difference between the third and the first steps of TPS nanoribbons oxidation reaction. The sulfur vacancy site is highlighted by black circle.

Structure	Atomic structure	$E_3 - E_1$ , eV			
		$Ta_2Pd_3S_8$	$Ta_2Pd_3Se_8$	$Ta_2Pt_3S_8$	$Ta_2Pt_3Se_8$
4		-0.42	1.35	-0.52	1.09
6		-1.22	0.58	-1.15	0.56

## SII. Electronic properties and structures of defected TPS nanoribbons.

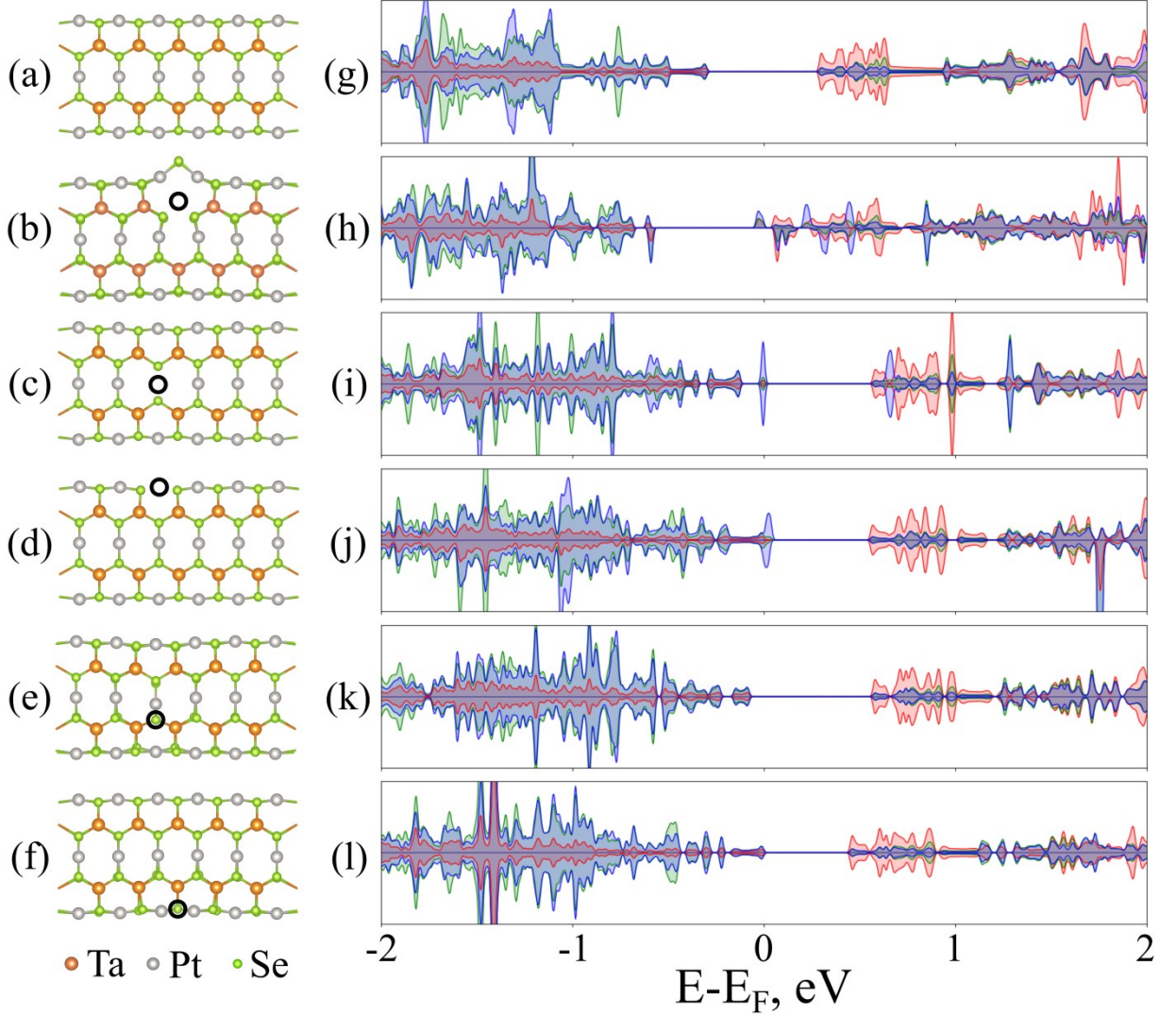


Figure S1. (a)-(f) Optimized atomic structures and (g)-(l) partial density of states for (a),(g) the pristine  $\text{Ta}_2\text{Pt}_3\text{Se}_8$  nanoribbon, (b),(h) nanoribbon with tantalum monovacancy, (c)-(d),(i)-(j) nanoribbon with platinum monovacancy located in the center (c),(i) and at the edge (d),(j) of the nanoribbon, (e)-(f), (k)-(l) nanoribbon with selenium monovacancy located in the center (e),(k) and at the edge (f),(l) of the nanoribbon. Vacancy sites are highlighted by black circles. Red lines correspond to the contribution from tantalum atoms, green lines – from the platinum atoms, blue lines – from the selenium atoms. The Fermi level is set to zero.

The partial density of states for defected  $\text{Ta}_2\text{Pt}_3\text{Se}_8$  nanoribbon is presented in Figure S1h-l. In the case of tantalum monovacancy the nanoribbon becomes a half-metal: for the majority spins channel the nanoribbon is metallic (the defect level is formed at about 0.04 eV below the CBM), for the minority spins channel the structure is semiconducting with a band gap of 0.64 eV. The presence of platinum monovacancy in both positions leads to the appearance of one defected state located in the band gap at about 0.12 eV and 0.02 eV above the VBM in the case of monovacancy located in the center and at the edge of the NR, respectively. Selenium monovacancies do not lead to the appearance of new states in the band gap, however, it should be noted that in the case of selenium vacancy located in the center of the NR the band gap increases and becomes equal to 0.64 eV, in the case of vacancy situated at the edge of the NR the band gap decrease and becomes equal to 0.45 eV.

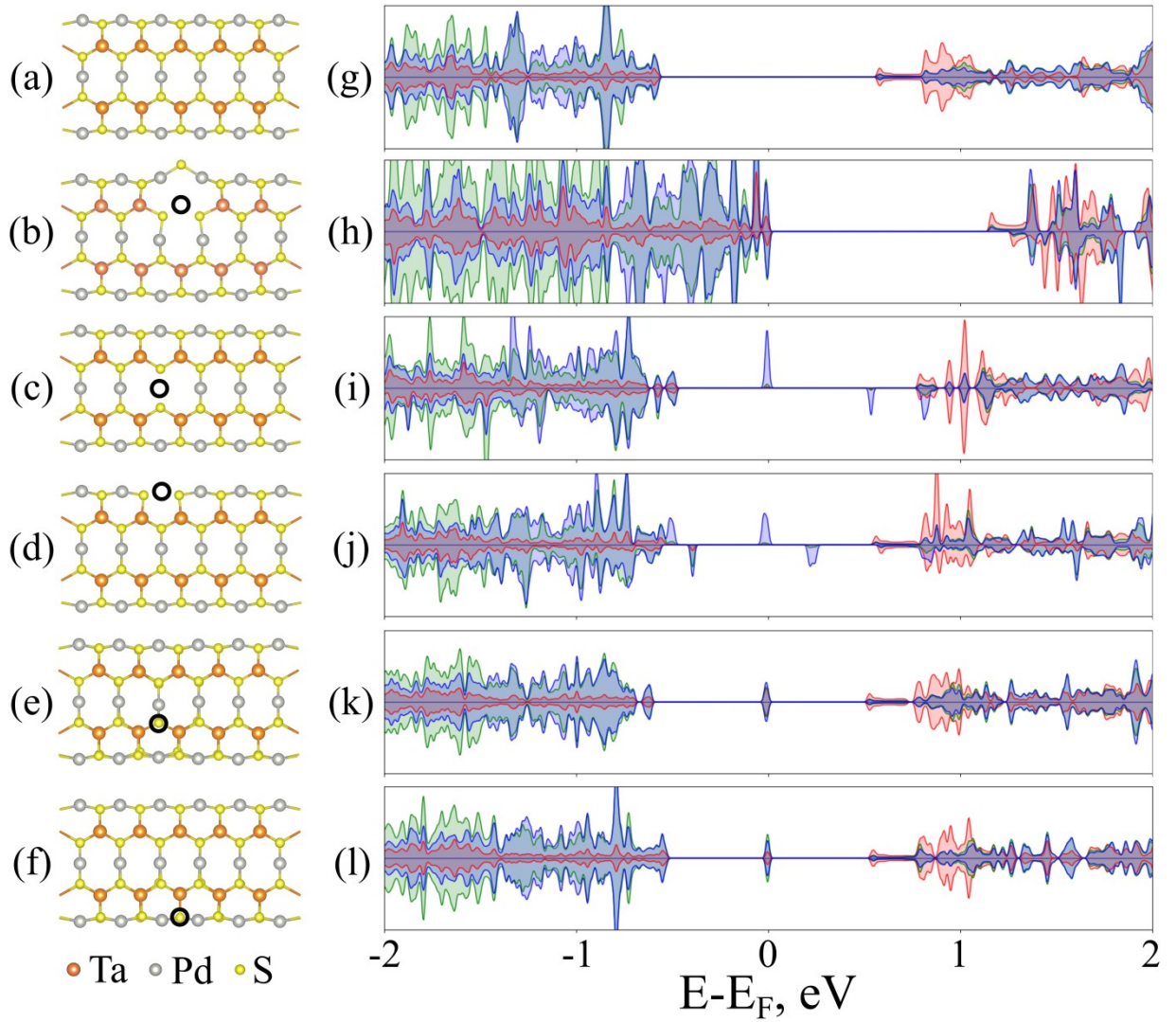


Figure S2. (a)-(f) Optimized atomic structures and (g)-(l) partial density of states for (a),(g) the pristine  $\text{Ta}_2\text{Pd}_3\text{S}_8$  nanoribbon, (b),(h) nanoribbon with tantalum monovacancy, (c)-(d),(i)-(j) nanoribbon with palladium monovacancy located in the center (c),(i) and at the edge (d),(j) of the nanoribbon, (e)-(f), (k)-(l) nanoribbon with sulfur monovacancy located in the center (e),(k) and at the edge (f),(l) of the nanoribbon. Vacancy sites are highlighted by black circles. Red lines correspond to the contribution from tantalum atoms, green lines – from the palladium atoms, blue lines – from the sulfur atoms. The Fermi level is set to zero.

The partial density of states for defected  $\text{Ta}_2\text{Pd}_3\text{S}_8$  nanoribbon is presented in Figure S2h-l. In the case of tantalum monovacancy the nanoribbon remains semiconductor. In the case of palladium vacancy located in the center of the nanoribbon a single defected state located at about 0.48 eV and 1.01 eV above the VBM for the majority and minority spins, respectively, is formed. In the case of palladium vacancy at the edge of the NR two defected state are formed: the first one is located close at about 0.02 and 0.17 eV above the VBM and the second state is situated at about 0.54 eV and 0.43 eV below the CBM for the majority and minority spins, respectively. The presence of sulfur monovacancy in the  $\text{Ta}_2\text{Pd}_3\text{S}_8$ -NR structure leads to the appearance of a single defected state located close to Fermi energy at about 0.60 eV and 0.52 eV above the VBM for vacancy located in the center and at the edge of the NR.

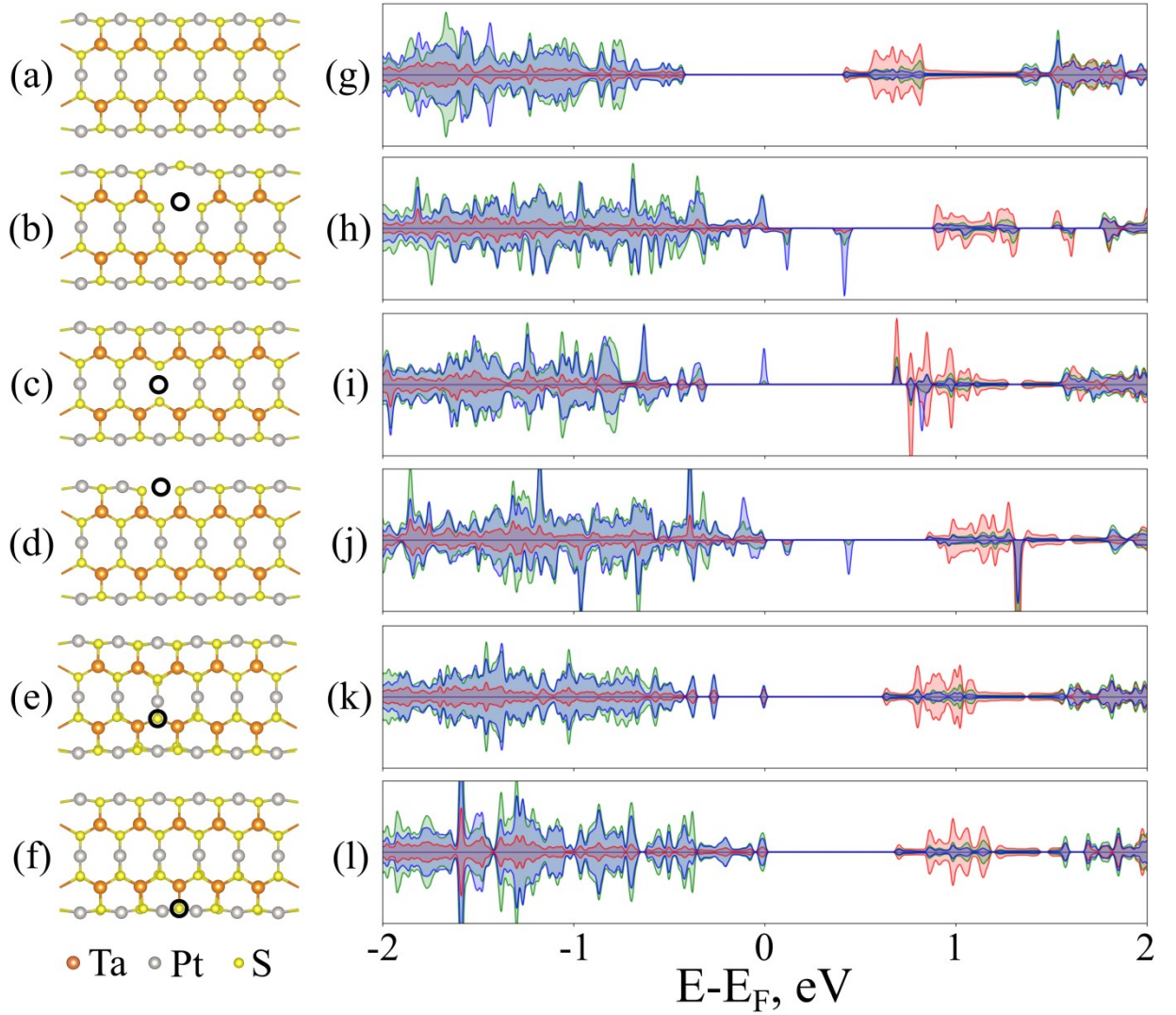


Figure S3. (a)-(f) Optimized atomic structures and (g)-(l) partial density of states for (a),(g) the pristine Ta<sub>2</sub>Pt<sub>3</sub>S<sub>8</sub> nanoribbon, (b),(h) nanoribbon with tantalum monovacancy, (c)-(d),(i)-(j) nanoribbon with platinum monovacancy located in the center (c),(i) and at the edge (d),(j) of the nanoribbon, (e)-(f), (k)-(l) nanoribbon with sulfur monovacancy located in the center (e),(k) and at the edge (f),(l) of the nanoribbon. Vacancy sites are highlighted by black circles. Red lines correspond to the contribution from tantalum atoms, green lines – from the platinum atoms, blue lines – from the sulfur atoms. The Fermi level is set to zero.

The partial density of states for defected Ta<sub>2</sub>Pt<sub>3</sub>S<sub>8</sub> nanoribbon is presented in Figure S3h-l. In the case of tantalum monovacancy the nanoribbon becomes a half-metal. For the majority spins channel the nanoribbon is metallic, the defect level is formed at about 0.23 eV above the VBM. For the minority spins channel the structure is semiconducting with a band gap of 0.86 eV. In the case of platinum vacancy located in the center and at the edge of the NR two defected state are formed for the majority spins: the first one is located close to Fermi energy at about 0.31 and 0.11 eV above the VBM, the second state is situated at about 0.06 eV and 0.46 eV below the CBM, respectively. The presence of sulfur monovacancy in the Ta<sub>2</sub>Pt<sub>3</sub>S<sub>8</sub>-NR structure leads to the appearance of a single defected state located at about 0.26 eV and 0.04 eV above the VBM for vacancy located in the center and at the edge of the NR.